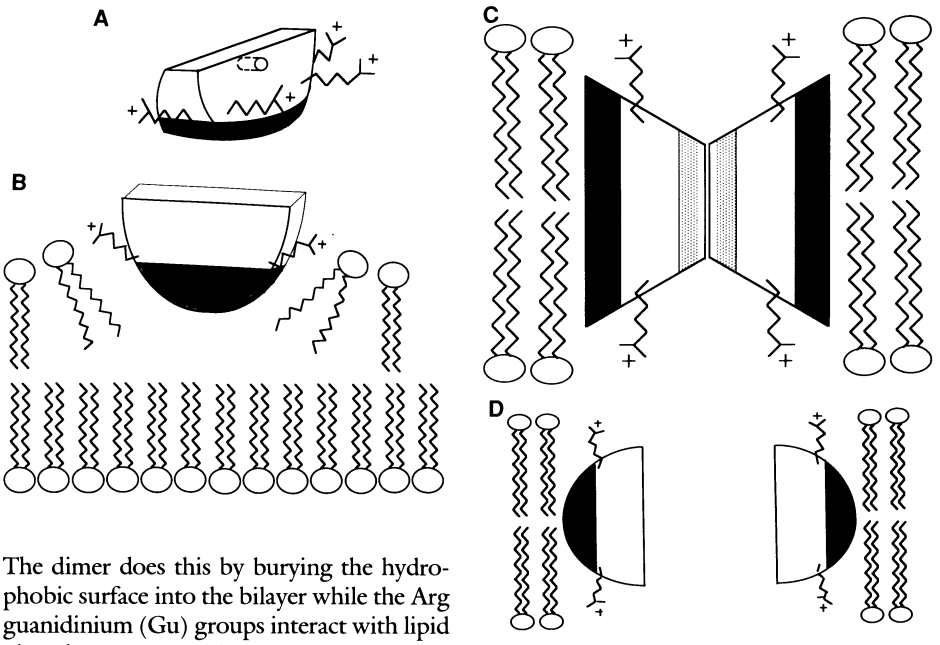

Fig. 3. (**A**) Schematic representation of the dimer basket. The top is hydrophilic, and the base is hydrophobic (shaded). Six flexible Arg residues are distributed around the middle. The solvent mini-channel is indicated. The local twofold is vertical. (**B**) Wedge hypothesis. The hydrophobic surface of the dimer is buried into the lipid bilayer, disrupting the lipid-lipid interactions and perhaps permeabilizing the membrane. (**C**)) Dimer-pore hypothesis. Two dimers stack top to top with their bottom hydrophobic surfaces (shaded) facing lipid tails. Association of the hydrophilic top surfaces is stabilized by charge complementarity. Two solvent mini-channels (stipled) cross the bilayer. (**D**) General-pore hypothesis. This cross section shows just two defensin dimers. In order to complete the pore, more dimers must be added in front and back. Modeling suggests that at least four dimers are required to complete this type of pore, which could include many defensin molecules and become very large.

three ways in which defensin molecules might interact with and permeabilize a lipid bilayer. A wedge effect, like that proposed for the permeabilization of membranes by melittin and lysolecithin (*31*), might result from the amphiphilicity of the dimer basket. A cluster of four hydrophobic side chains on the bottom of the basket (Figs. 1C and 3A) provides a hydrophobic patch of 344 Å^2 of solvent-accessible surface area that is surrounded, further up the basket, by the ring of six Arg side chains. In the wedge hypothesis, the HNP-3 dimer disrupts the membrane by distorting lipid-lipid interactions. The dimer does this by burying the hydrophobic surface into the bilayer while the Arg guanidinium (Gu) groups interact with lipid phosphate groups (Fig. 3B).

Two other possible mechanisms emerge from the structure, both of which involve pore formation. One of these, the dimer pore, makes use of the solvent mini-channel seen in the crystal structure (Fig. 1, D and E). In this model, two dimers assemble in the membrane with their polar tops toward each other and apolar bases facing lipid tails (Fig. 3C). There is some charge complementarity at this putative dimer-dimer interface, especially involving the ion pair Arg^6 and Glu^{14}. The side chains of the six "equatorial" Arg residues move to bind lipid head groups. In this configuration, two of the solvent mini-channels seen in the crystal structure completely span the bilayer.

The other, general-pore, hypothesis also has dimers completely spanning the membrane, but now rotated by ~90° from the "dimer-pore" orientation and with the polar top surface lining the pore (Fig. 3D). The same hydrophobic dimer surface contacts lipid tails, and Arg side chains have again moved to bind head groups. Simple modeling suggests that at least four dimers are required to form this type of pore, which could conceivably become very large and include many defensin dimers.

At this stage it is not possible to tell which, if any, of these three ideas are correct. Indeed they might all have elements of correctness, since a wedge interaction could be the forerunner of either of the other two "pore" models. The concentration dependence of defensin activity (*10*) might reflect transitions from wedge to dimer-pore to general-pore mechanisms.

Each of the three models requires burying essentially the same hydrophobic surface against the lipid aliphatic chains, binding of the same Arg Gu functions to lipid head groups, and exposing the same hydrophilic surface to a suitable environment. Consequently, consideration of the various defensin sequences may support each model, but will not in general allow us to choose among them. The greatest challenge to the three hypotheses is the presence of Asp^{18} in NP-3b, which in all the models is buried in the middle of the membrane. Consideration of Arg^{16} suggests that this is not a fatal flaw in

Table 2. Refinement statistics for the atomic model in which the restrained least squares program of Hendrickson was used (*38*).

Refinement parameter	Value
Resolution range (Å)	1.9–10.0
Reflections (no.)	4448
R factor*	0.190
Protein atoms included (no.)	270
Protein atoms missing (no.)	12
Water molecules included (no.)	44
B factor: Wilson plot (2.5–1.9 Å) (Å^2)	15.6
B factor: Molecule A average (Å^2)	14.5
B factor: Molecule B average (Å^2)	17.9
B factor: Solvent average (Å^2)	38.3
(1–2) Bond distances (Å)†	0.019 (0.020)
(1–3) Angle distances (Å)	0.049 (0.040)
(1–4) Distances (Å)	0.045 (0.050)
Planarity (Å)	0.014 (0.020)
Chiral volumes (Å^3)	0.180 (0.150)
Nonbonded contacts (Å)	
Single torsion	0.204 (0.500)
Multiple torsion	0.274 (0.500)
Possible hydrogen bonds	0.181 (0.500)
Conformation torsion angles (degrees)	
Planar (0°, 180°)	2.8 (3.0)
Staggered (±60°, 180°)	18.2 (15.0)
Orthonormal (±90°)	28.8 (20.0)
Isotropic temperature factors (Å^2)	
Main-chain bond	0.991 (1.000)
Main-chain angle	1.720 (1.500)
Side-chain bond	1.565 (1.000)
Side-chain angle	2.427 (1.500)

*$R = (\sum | F_{obs} | - | F_{calc} |)/\sum | F_{obs} |$. †The values are the rms deviations; the target σ values are given in parentheses.